Sliding Window and Filterbank Utilization on Riemannian Geometry

Fatih ALTINDİŞ
Electrical and Computer Engineering
Abdullah Gül University
Kayseri, Turkey
fthaltindis@gmail.com

Bülent YILMAZ
Electrical and Electronics Engineering
Abdullah Gül University
Kayseri, Turkey
bulent.yilmaz@agu.edu.tr

2022 International Conference on INnovations in Intelligent SysTems and Applications (INISTA) | 978-1-6654-9810-4/22/$31.00 ©2022 IEEE | DOI: 10.1109/INISTA55318.2022.9894208

***Abstract*— Riemannian geometry-based signal processing approaches on EEG signals provides similar decoding performance compared to *state-of-the-art* methods. However, Riemannian geometry framework requires predefine EEG signal epoch that is to be used in the analysis. Sliding window approach that operates in Riemannian geometry proposed to enable use of EEG signals without constrained by the record length. Decoding performance of tangent space mapping was increased more than 6% in overall accuracy compared the previous study's results. Instead of using single band-pass filter, utilization of filterbank is proposed to increase decoding performance. Distance based Riemannian classifier's overall performance were increased by 5% compared to standard Riemannian geometry approach.**

Keywords—Riemannian Geometry, Tangent Space Mapping, Brain-Computer Interface, EEG

I. INTRODUCTION

Brain computer interfaces (BCIs) aim to monitor and decode ongoing brain activity in order to produce feedback messages to users or to help operation of predefined tasks [1]. Ideally, monitoring of the users should be completed without interfering their daily lives and information gathering should be fast, accurate and concise. Electroencephalography (EEG) signals are recorded from set of electrodes that are placed on user's scalp for acquiring ongoing brain activity. BCI system and its users can be trained to respond brain activity that emerges with synchronous stimulation such as visual evoked potentials. Alternatively, users can be trained to arouse certain EEG activity in order to convey a message or operate a device (mouse cursor, wheelchair etc.) without requiring and stimulation (asynchronously) [2-5].

Recently introduced Riemannian geometry-based signal processing techniques enable avant-garde way to process and analyze EEG signals to extract information [6-8]. While Riemannian geometry-based approaches allow simpler and faster signal processing pipeline compared to *state-of-the-art* methods, decoding performance of this approach outscores *state-of-the-art* methods. In this approach, properties of symmetric positive definite (SPD) matrices and Riemannian distance between SPD matrices are exploited to extract information from EEG signals.

In this study, we focused on two points: creation of SPD matrices from EEG signals and classification of SPD matrices. We investigated parameters that are effective on creating SPD from EEG signals, which eventually have profound effect on decoding performance. Next, we analyzed the effect of dividing EEG signals into multiple sub-bands and use them separately for creating SPD. Following that, we compared different strategies to combine Riemannian geometry features extracted from multiple sub-bands. Finally, we compared and discussed decoding performance of these adjusted approaches with standard Riemannian geometry methods.

II. MATERIALS AND METHODS

A. Riemannian Geometry

We would like to briefly introduce mathematical background of Riemannian geometry in order to lay a groundwork for our contribution. Riemannian geometry is thoroughly explained and discussed in studies of Barachant et al. [7], which is worth to take note of for the deeper understanding of the topic and grasping of the concept.

EEG signals that are taken from M channels, can be represented with a matrix $\boldsymbol{X}_i \in \mathbb{R}^{M\times N}$, where i represent trial number, M represents number of channels and N represents number of data samples. Each channel (row) of $\boldsymbol{X}_i$ is bandpass filtered and centered to zero in the preprocessing step, then sample covariance matrix (SCM) of each trial is estimated using equation 1 (T denotes transpose).

$$\boldsymbol{P}_i = \frac{1}{N-1}\boldsymbol{X}_i\boldsymbol{X}_i^T \in \mathbb{R}^{M\times M} \tag{1}$$

SCMs are square matrices ($\boldsymbol{P}_i$) that are symmetric along the diagonal and all elements are positive, consequently satisfies SPD matrix features. Once each EEG trial is used to create sample covariance matrices, Riemannian geometry comes into play. Instead of using Euclidean distance metrics, Riemannian distance features are used to find mean or distance between $\boldsymbol{P}_i$ matrices. Riemannian distance between two SPD matrices is calculated as in equation 2. Note that, each $\boldsymbol{P}_i$ matrix represents a single point in the manifold.

$$\delta_R(\boldsymbol{P}_1,\boldsymbol{P}_2) = \|\mathrm{Log}(\boldsymbol{P}_1^{-1}\boldsymbol{P}_2)\|_F$$
$$= \left\|\mathrm{Log}(\boldsymbol{P}_1^{-1/2}\boldsymbol{P}_2\boldsymbol{P}_1^{-1/2})\right\|_F = [\textstyle\sum_{i=1}^{M}\log^2\lambda_i]^{1/2} \tag{2}$$

The term $\|\cdot\|_F$ is Frobenius norm of a matrix, λ_i are the eigenvalues of $\mathbf{P}_1^{-1}\mathbf{P}_2$ and $\mathrm{Log}(\cdot)$ is matrix logarithm [9]. Riemannian distance $\delta_R(\cdot)$ is the minimum length of a curve that connects two points on the manifold and can be referred as 'geodesic'.

Riemannian mean of K matrices that lie on the same manifold is estimated by solving the following optimization problem in equation 3, where $\boldsymbol{G}$ is Riemannian mean of SPD matrices, which is also an SPD matrix itself.

$$\arg\min_{\boldsymbol{G}} \ \tfrac{1}{K}\textstyle\sum_{i=1}^{K}\delta_R^2(\boldsymbol{P}_i,\boldsymbol{G}) \tag{3}$$

Once mean of the manifold estimated, each point can be projected to the new linear (Euclidean) space using a tangent

978-1-6654-9810-4/22/$31.00 ©2022 IEEE

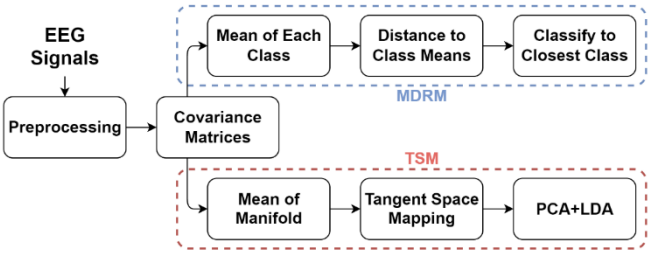

Figure 1. Signal processing pipeline of MDRM and TSM methods

plane $\mathcal{T}(M)$ that goes through $\boldsymbol{G}$ using the equation 4. Since M-channel EEG signals are used to create SPD matrices at the first place, resulting tangent space features will have dimension of $M(M+1)/2$. Note that $upper(\cdot)$ is an operator to vectorize upper triangular part of the matrix.

$$\mathcal{T}(M) = \boldsymbol{s}_i = upper\left(\mathrm{Log}\left(\boldsymbol{G}^{-1/2}\boldsymbol{P}_i\boldsymbol{G}^{-1/2}\right)\right),$$
$$\boldsymbol{s}_i \in \mathbb{R}^{M(M+1)/2} \tag{4}$$

Riemannian mean of each class can be used to classify unlabeled instances in the manifold based on their distance to each class mean, resulting a distance-based classifier called minimum distance to Riemannian mean (MDRM) [10]. All the processing steps after creating SPD matrices, are completed in Riemannian space in this approach.

Alternatively, tangent space mapping (TSM) approach projects all the points into linear space before the classification step and completes training and testing on the linear space. On top of linear discriminant analysis (LDA), utilization of principal component analysis (PCA) to TSM features yield better decoding performance than MDRM classifier [10, 11]. We are concluding this brief background introduction by summarizing signal processing pipeline of both MDRM and TSM based approaches in figure 1.

B. Sliding Window on Riemannian Geometry

Sample covariance matrix (SCM) estimation step of Riemannian geometry-based signal processing pipeline is examined carefully to understand how it affects classification performance, when longer/shorter EEG signal epochs are used for estimation of SCMs. Depending on the task, emergence period and duration of certain activities on EEG can change [12]. Thus, width of EEG epoch that is to be used to estimate SCM, is vital to embed related task information into SCMs. Additionally, it is important to choose correct time interval for EEG epochs to capture only task related activities. An ordinary EEG experiment that is designed to record motor intention activities consist of resting, imagination and relaxation periods for each trial as shown in Figure 2.

Three different epoch selection is shown in the given figure just to represent possible time interval choices from a single EEG trial. It can be seen that, if the W1 or W3 time intervals are chosen to estimate SCM, some of the data would come from relaxation or rest period. Preferably, W2 time interval only use imagination related part of signals. Still, even W2 time interval is not perfect to capture task related data since it leaves some of the task-related part of the signals out. But then, increasing the width of the window to capture whole task period in a single window is not preferred, because task related information vanishes, and background data of EEG signals becomes prominent as the windows get wider. This creates a trade-off between opting for wider windows to include as much task-related data as possible and opting for narrower windows to eliminate non-task related background data.

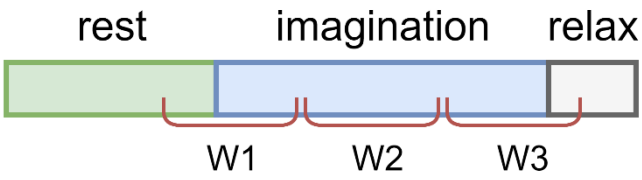

Figure 2. Usual experiment paradigm for recoding motor imagery activity

Here, we propose to implement sliding window approach to estimate multiple SCMs from a single EEG trial and then find the mean of these SCMs to represent that particular EEG trial with a new SPD matrix. There are two advantages of the sliding window approach, it allows to use all imagination period, and to use narrower windows to capture ongoing task-related activity better. Window length and slide rate (of the window) are the two parameters that are effective on the estimated SCMs in this approach. Since mean and distance metrics are constrained by Riemannian geometry, Riemannian means of the sliding window SCMs are estimated for each trial. Consequently, each trial is represented by one SPD matrix similar to standard approach, but this new SPD matrices are different from straight-forward estimation of SCMs. Regardless of MDRM or TSM, remaining steps of the processing is exactly the same with chosen method.

Proposed sliding window approach has key parameters which are window length (W) and slide rate (s). Window length is expressed in terms of seconds and slide rate is expressed in terms of percentage that window is slid. For instance, 2 seconds sliding window with 20% slide rate means, window is slid 0.4 seconds.

C. Filterbank Approach

Second proposal in this study is the utilization of filterbank at the preprocessing step in order to break down EEG signal into sub-bands and perform the rest of the processing steps on each sub-band independently. Filter-bank approach is expressed in the equation 5, where $\boldsymbol{X}_{ij}$ is i-th EEG trial filtered with j-th filter, j represents filter from filterbank and F is total number of filters in the filterbank.

$$\boldsymbol{X}_{ij} \in \mathbb{R}^{M\times N},\ j \in \{1,\dots,F\} \tag{5}$$

Distinctively, utilization of filterbank produces multiple Riemannian manifolds (sub-manifolds) for where each manifold belongs to filtered EEG signals of one filter from filterbank. This requires a different classification strategy than MDRM that takes all sub-manifolds into consideration. Here we implemented two approaches to classify unlabeled instances: majority voting (MJV) and total distance to Riemannian means (TDRM). In majority voting, each trial classified to the class that has the highest number of votes coming from based on the MDRM prediction of each sub-manifold. TDRM is a distance-based classifier, where distances between instance to each class mean on sub-manifolds are summed up and final prediction is made based on the total distance. Equation 6 summarizes total distance to Riemannian means classification approach, for i-th instance $\boldsymbol{P}_{ij}$, its distance to each class means ($\boldsymbol{M}_{cj}$) on the sub-manifolds are summed to find the minimum distance, where c represents the class $c \in \{1,\dots,C\}$.

TABLE I. DISPERSION RATIO OF SLIDING WINDOW OVER FIXED WINDOW

Window Length	Slide rate	Left Hand	Right Hand	Foot	Tongue	Manifold
1 second	20 %	0.94	0.94	0.91	0.95	0.95
	50 %	0.90	0.90	0.87	0.91	0.90
	70 %	0.96	0.96	0.93	0.96	0.95
1.5 second	20 %	1.03	1.04	1.00	1.05	1.04
	50 %	1.00	1.00	0.97	1.02	1.01
	70 %	1.04	1.04	1.01	1.06	1.04
2 seconds	20 %	1.06	1.07	1.03	1.09	1.08
	50 %	0.99	0.99	0.96	1.01	1.00
	70 %	1.09	1.10	1.07	1.11	1.09

$$\arg\min_{\boldsymbol{M}_c} \sum_{j=1}^{F} \delta_R^2\left(\boldsymbol{P}_{ij}, \boldsymbol{M}_{cj}\right) \tag{6}$$

In this study, we used two different filterbank, one with 3 filters that are 8-15 Hz, 15-22 Hz and 22-30 Hz band-pass filters in it. The second filterbank has 13 filters that are 8-10 Hz, 9-11 Hz, 10-12 Hz, 11-13 Hz, 12-14 Hz, 13-15 Hz, 15-20 Hz, 17-22 Hz, 19-24 Hz, 21-26 Hz, 23-28 Hz, 25-30 Hz, 27-32 Hz.

D. Dataset and Software

BCI IV competition dataset 2a, which is one of the most preferred dataset among recent Riemannian geometry-based studies for benchmarking, is used to compare and verify proposed approach's results. This dataset has 22-channel EEG recordings that belong to 4-class motor imagery (left hand, right hand, foot, tongue) data taken from 9 different subjects [13]. Each trial in this dataset starts with 2 seconds of resting period followed by 4 seconds of motor imagination period. We used entire imagination time interval (4 seconds) of each trial to estimate SCMs for standard MDRM approach (by standard approach we mean use of fixed time window). Sliding window approach covered these 4 seconds of imagination period as explained above in the sliding window sub-section and returned a single SPD matrix that is the Riemannian mean of all of the windowed SCMs for the corresponding trial.

All the data processing and Riemannian geometry operations were performed on Python with the help of PyRiemann and Scikit-Learn libraries [14, 15].

III. RESULTS

We have estimated dispersion of instances around class means to compare sliding window approach versus standard approach that is proposed by Barachant et al. [7]. Dispersion of data points in the Riemannian manifold can be estimated with equation 7 as follows.

$$d = \frac{1}{K}\sum_{i=1}^{K} \delta_R^2(\boldsymbol{P}_i, \boldsymbol{M}_c) \tag{7}$$

Then, we take the ratio of both approaches' dispersions to see which one is scattered more compared to the other. This dispersion ratio of sliding windowed approach to standard approach can be used to understand how much EEG trials are scattered in the Riemannian manifold [16]. If the dispersion ratio is below 1, it means EEG trials are less scattered around class means in sliding windowed approach than the standard approach. Table 1 below shows comparison of average dispersion ratios (across 9 subjects) for different set of window length and slide rate values.

Values on table 1 show that dispersion increases when 20% or 70% sliding rate is used in sliding window approach. Additionally, as window length gets wider, dispersion of the instances around class means increases. Apart from the dispersion rates of classes, distance between class means is measured. Once the class means of four classes in the dataset were estimated, distance between each class is measured. This information is valuable because, MDRM classifier operates on distance metrics (Riemannian) and if the class means were landed apart from each other on the manifold when the sliding window approach is used, consequently classification performance of the MDRM classifier should increase as well. Table 2 shows how much the distance between each class pair is changed compared to standard approach.

Next, we implemented two set of filterbank to the preprocessing step as previously explained. Remaining steps of the processing pipeline was the same as before in terms of estimation of SCMs and Riemannian mean. First filterbank has 3 filters and the second has 13 filters, meaning that at the last stage there were 3 manifolds for the first filterbank and there were 13 manifolds for the second filterbank. Majority voting and total distance to Riemannian mean classification strategies are used in the last step as explained in the previous section. Table 4 shows classification results of filterbank approach for both MDRM and TSM approaches.

Classification results in table 4 show that, utilization of filterbank before the estimation of SCMs increases classification performance for all subjects. In fact, utilization of sliding window on top of filterbank further increases the classification performance. Interestingly, filterbank approach significantly decreased classification performance, when fixed window is used for SCM estimation. Overall classification performance is improved 6% across all subjects with filterbank utilization and sliding window approach to estimate SCM from each EEG trial.

TABLE II. CLASS MEANS DISTANCE CHANGE RATIO OF SLIDING WINDOW OVER FIXED WINDOW

Window Length	Slide rate	LvR	LvF	LvT	RvF	RvT	FvT	Av
1 second	20 %	1.14	1.11	1.08	1.09	1.08	1.04	1.09
	50 %	1.07	1.05	1.03	1.04	1.03	1.01	1.04
	70 %	1.09	1.04	1.02	1.03	1.02	0.98	1.03
1.5 second	20 %	1.13	1.10	1.06	1.08	1.07	1.03	1.08
	50 %	1.09	1.06	1.03	1.05	1.04	1.00	1.04
	70 %	1.08	1.03	1.01	1.02	1.02	0.98	1.02
2 seconds	20 %	1.06	1.04	1.00	1.03	1.02	0.98	1.02
	50 %	1.02	1.01	0.97	1.01	0.99	0.95	0.99
	70 %	1.01	0.99	0.96	0.99	0.98	0.94	0.98

[a.] L – Left Hand, R – Right Hand, F – Foot, T – Tongue

TABLE III. CLASSIFICATION RESULTS OF 20 % SLIDE RATE SLIDING WINDOW FOR MDRM AND TSM METHODS

	MDRM				TSM			
Subjects	**Barachant [7]**	**1 second window**	**1.5 second window**	**2 seconds window**	**Barachant [7]**	**1 second window**	**1.5 second window**	**2 seconds window**
A01	77.80	79.18	78.65	79.00	80.50	85.14	84.69	84.52
A02	44.10	51.73	53.82	54.35	51.30	66.02	64.52	63.57
A03	76.80	76.55	76.20	76.38	87.50	90.12	89.87	90.15
A04	54.90	54.87	57.65	56.78	59.30	69.06	69.33	68.88
A05	43.80	37.86	37.86	36.99	45.00	49.16	48.61	48.43
A06	47.10	46.71	47.23	45.31	55.30	59.58	59.68	59.59
A07	72.00	75.37	76.41	75.54	82.10	90.67	90.79	90.12
A08	75.20	78.27	77.23	77.58	84.80	91.20	90.05	89.39
A09	76.60	74.49	74.67	73.80	86.10	83.86	83.95	82.86
Average	63.14	63.89	64.41	63.97	70.21	76.09	75.72	75.28

IV. DISCUSSION

In this study, we propose two intermediate steps to signal processing pipeline of the Riemannian geometry-based analysis of EEG signals in order to increase the decoding performance without compromising advantages of Riemannian geometry. We started by introducing sliding window method that exploits Riemannian geometry for producing an SPD matrix that will represent single EEG trial, while incorporating all of the information from the region of interest regardless of its duration. Sliding rate and window length are the two parameters that are effective on the estimated SPD matrices with sliding window method. Quantification of the proposed sliding window method and the effect of these two parameters were investigated by comparing and measuring the change of dispersion and distance between class means.

It is expected that less dispersion among the same class instances provides better classification performance for distance-based classifiers. Despite having higher dispersion in sliding window approach compared to standard approach (table 1), where fixed time window is used to estimate SCM, classification performance is better in sliding window approach. The reason behind this performance increase became evident in table 2 that shows the distance change between class means. As we briefly introduced in section 2, MDRM classifier estimates mean of each class and label new instances based on their distance to these class means. When sliding window is utilized, mean of classes went further away from each other. This allowed to nudge instances that are located at the boundary regions apart from each other. Still, increase in the dispersion dilutes this advantage and MDRM classification performance stays at similar level as it can be seen from table 3. On the other hand, it helps to improve TSM method's overall classification performance by 6%. In fact, classification accuracy of 4 subjects (A02, A04, A07, A08) increased 8-15% compared to the standard TSM approach results shared by [7].

Next, we utilized filterbank instead of single band-pass filter at the preprocessing step and performed MDRM or TSM on each filter's output signal. We applied two different classification strategy at the last step for labeling test data. Essentially, total distance to Riemannian mean corresponds to average distance of each instance across the manifolds. Usually, use of single band-pass filter excludes subject specific changes on different frequency bands; therefore, some information may go missing for subjects (A02 and A04). However, when filterbank is utilized, each sub-band is evaluated independently from each other, which helped to increase decoding performance of subjects who performed poorly otherwise. Notably, sliding window approach plays a key role for high classification accuracy of the filterbank approach. In table 4, it can be seen that, fixed window approach results in extremely poor classification performances on all subjects in contrast to sliding window approach.

In brief, compared the recent studies that are focused on improving TSM method's decoding performance by implementing further techniques to select features, sliding window approach offers simpler and faster way to improve classification accuracy [17, 18]. Additionally, sliding window allows to cover whole signal epoch that belongs to the task without compromising decoding performance or real-time compatibility of the signal processing pipeline.

Performance of the sliding window approach against artefacts and noises is yet to be explored. Filterbank approach allows partitioning of the EEG signals into sub-bands and working on multiple manifolds. Another potential research direction can be exploring different options at the combination of the features that are extracted from sub-band manifolds.

TABLE IV. CLASSIFICATION RESULTS OF FILTERBANK APPROACH

	3 filterbank					13 filterbank				
	Sliding Window		**Fixed Window**			**Sliding Window**		**Fixed Window**		
Subjects	**MJV**	**TDRM**	**MJV**	**TDRM**	**TSM**	**MJV**	**TDRM**	**MJV**	**TDRM**	**TSM**
A01	79.17	84.20	58.68	65.45	87.50	81.42	83.68	63.89	67.36	84.37
A02	51.74	55.03	42.53	46.18	64.26	48.96	53.99	43.06	47.40	58.81
A03	68.06	75.87	46.18	55.38	88.71	77.60	82.99	53.13	57.64	91.68
A04	56.77	63.54	35.42	39.06	73.07	59.20	63.72	35.42	36.98	55.40
A05	40.80	45.14	28.99	30.73	52.73	44.62	46.18	30.03	33.16	39.25
A06	44.44	47.57	36.11	36.63	57.79	47.92	49.65	37.33	40.10	50.19
A07	76.56	81.77	51.74	54.51	90.28	79.86	83.85	52.26	55.21	79.68
A08	73.09	78.13	55.90	57.12	90.96	76.74	80.21	57.12	60.24	87.52
A09	70.31	72.57	54.17	55.73	84.03	72.92	73.96	54.69	56.08	80.92
Average	62.33	67.09	45.52	48.98	76.59	65.47	68.69	47.43	50.46	69.76

REFERENCES

[1] S. J. Luck, "Quantifying ERP Amplitudes and Latencies," (in English), *Introduction to the Event-Related Potential Technique, 2nd Edition,* pp. 283-307, 2014. [Online]. Available: <Go to ISI>://WOS:000344667700010.

[2] A. Kubler, B. Kotchoubey, J. Kaiser, J. R. Wolpaw, and N. Birbaumer, "Brain-computer communication: unlocking the locked in," *Psychol Bull,* vol. 127, no. 3, pp. 358-75, May 2001, doi: 10.1037/0033-2909.127.3.358.

[3] E. W. Sellers and E. Donchin, "A P300-based brain-computer interface: initial tests by ALS patients," *Clin Neurophysiol,* vol. 117, no. 3, pp. 538-48, Mar 2006, doi: 10.1016/j.clinph.2005.06.027.

[4] G. R. Muller-Putz *et al.*, "Towards Non-Invasive EEG-based Arm/Hand-Control in Users with Spinal Cord Injury," (in English), *2017 5th International Winter Conference on Brain-Computer Interface (Bci),* pp. 63-65, 2017. [Online]. Available: <Go to ISI>://WOS:000403612000018.

[5] C. H. Han, K. R. Muller, and H. J. Hwang, "Brain-Switches for Asynchronous Brain-Computer Interfaces: A Systematic Review," (in English), *Electronics-Switz,* vol. 9, no. 3, Mar 2020, doi: 10.3390/electronics9030422.

[6] A. Barachant, S. Bonnet, M. Congedo, and C. Jutten, "Riemannian Geometry Applied to BCI Classification," in *Latent Variable Analysis and Signal Separation*, Berlin, Heidelberg, V. Vigneron, V. Zarzoso, E. Moreau, R. Gribonval, and E. Vincent, Eds., 2010// 2010: Springer Berlin Heidelberg, pp. 629-636.

[7] A. Barachant, S. Bonnet, M. Congedo, and C. Jutten, "Multiclass brain-computer interface classification by Riemannian geometry," *IEEE Trans Biomed Eng,* vol. 59, no. 4, pp. 920-8, Apr 2012, doi: 10.1109/TBME.2011.2172210.

[8] M. Congedo, A. Barachant, and A. Andreev, "A New Generation of Brain-Computer Interface Based on Riemannian Geometry," p. arXiv:1310.8115.

[9] F. Yger, M. Berar, and F. Lotte, "Riemannian Approaches in Brain-Computer Interfaces: A Review," *IEEE Trans Neural Syst Rehabil Eng,* vol. 25, no. 10, pp. 1753-1762, Oct 2017, doi: 10.1109/TNSRE.2016.2627016.

[10] M. Congedo, A. Barachant, and R. Bhatia, "Riemannian geometry for EEG-based brain-computer interfaces; a primer and a review," (in English), *Brain-Comput Interfa,* vol. 4, no. 3, pp. 155-174, 2017, doi: 10.1080/2326263x.2017.1297192.

[11] F. Lotte *et al.*, "A review of classification algorithms for EEG-based brain-computer interfaces: a 10 year update," (in English), *J Neural Eng,* vol. 15, no. 3, Jun 2018, doi: 10.1088/1741-2552/aab2f2.

[12] G. Pfurtscheller, "Spatiotemporal ERD/ERS patterns during voluntary movement and motor imagery," *Suppl Clin Neurophysiol,* vol. 53, pp. 196-8, 2000, doi: 10.1016/s1567-424x(09)70157-6.

[13] R. Leeb, G. Muller-Putz, A. Schlogl, and G. Pfurtscheller. *BCI Competition IV - Graz Dataset 2a*. [Online]. Available: http://www.bbci.de/competition/iv/#dataset2a

[14] A. Barachant, *pyRiemann v0.2.2*. Zenodo, 2015.

[15] F. Pedregosa *et al.*, "Scikit-learn: Machine Learning in Python," *Journal of Machine Learning Research,* vol. 12, pp. 2825-2830, 2011 2011.

[16] P. L. C. Rodrigues, C. Jutten, and M. Congedo, "Riemannian Procrustes Analysis: Transfer Learning for Brain-Computer Interfaces," (in English), *Ieee T Bio-Med Eng,* vol. 66, no. 8, pp. 2390-2401, Aug 2019, doi: 10.1109/Tbme.2018.2889705.

[17] X. Xie, Z. L. Yu, Z. Gu, J. Zhang, L. Cen, and Y. Li, "Bilinear Regularized Locality Preserving Learning on Riemannian Graph for Motor Imagery BCI," *IEEE Trans Neural Syst Rehabil Eng,* vol. 26, no. 3, pp. 698-708, Mar 2018, doi: 10.1109/TNSRE.2018.2794415.

[18] S. Li, X. Xie, Z. Gu, Z. L. Yu, and Y. Li, "Motor Imagery Classification based on Local Isometric Embedding of Riemannian Manifold," in *2019 14th IEEE Conference on Industrial Electronics and Applications (ICIEA)*, 19-21 June 2019 2019, pp. 2368-2372, doi: 10.1109/ICIEA.2019.8833878.